This article was downloaded by:
On: *18 January 2011*
Access details: *Access Details: Free Access*
Publisher *Taylor & Francis*
Informa Ltd Registered in England and Wales Registered Number: 1072954 Registered office: Mortimer House, 37-41 Mortimer Street, London W1T 3JH, UK

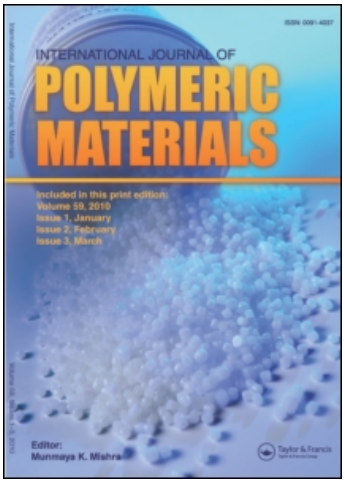

International Journal of Polymeric Materials
Publication details, including instructions for authors and subscription information:
http://www.informaworld.com/smpp/title~content=t713647664

Synthesis and Characterization of NiS/MnS Core-Shell Embedded Conducting Polyaniline Composite for Photovoltaic Application

T. R. Heera[a]; L. Cindrella[a]
[a] Department of Chemistry, National Institute of Technology, Tiruchirappalli, Tamil Nadu, India

Online publication date: 29 June 2010

To cite this Article Heera, T. R. and Cindrella, L.(2010) 'Synthesis and Characterization of NiS/MnS Core-Shell Embedded Conducting Polyaniline Composite for Photovoltaic Application', International Journal of Polymeric Materials, 59: 8, 607 — 621
To link to this Article: DOI: 10.1080/00914031003760725
URL: http://dx.doi.org/10.1080/00914031003760725

PLEASE SCROLL DOWN FOR ARTICLE

Full terms and conditions of use: http://www.informaworld.com/terms-and-conditions-of-access.pdf

This article may be used for research, teaching and private study purposes. Any substantial or systematic reproduction, re-distribution, re-selling, loan or sub-licensing, systematic supply or distribution in any form to anyone is expressly forbidden.

The publisher does not give any warranty express or implied or make any representation that the contents will be complete or accurate or up to date. The accuracy of any instructions, formulae and drug doses should be independently verified with primary sources. The publisher shall not be liable for any loss, actions, claims, proceedings, demand or costs or damages whatsoever or howsoever caused arising directly or indirectly in connection with or arising out of the use of this material.

International Journal of Polymeric Materials, 59:607–621, 2010
Copyright © Taylor & Francis Group, LLC
ISSN: 0091-4037 print/1563-535X online
DOI: 10.1080/00914031003760725

Taylor & Francis
Taylor & Francis Group

Synthesis and Characterization of NiS/MnS Core-Shell Embedded Conducting Polyaniline Composite for Photovoltaic Application

Downloaded At: 15:55 18 January 2011

T. R. Heera and L. Cindrella

Department of Chemistry, National Institute of Technology,
Tiruchirappalli, Tamil Nadu, India

Conducting polyaniline (Pani) films embedded with Co^{2+} doped, PVA-capped NiS/MnS core-shell particles as photoluminescent boosters have been developed and reported. The absorption and photoluminescence characteristics of the core-shell Pani have increased significantly. Film of the core-shell-Pani composite is n-type semiconductor with a band gap of 2.34 eV. Periodic arrangement of the nanoclusters of the core-shell in the continuous conductive polymer matrix with high carrier density (3.99×10^{16}) rates this material for photoelectrochemical applications. Solid-state photovoltaic cells with NiS/MnS-Pani as the electron conductor shows a I_{sc} of 0.14 mA/cm^2, V_{oc} of 382 mV and photo conversion efficiency of 1.25%.

Keywords composite materials, optical properties, polymer, semiconductor

INTRODUCTION

In recent years, there has been considerable interest in polymer-metal sulphide nanocomposites on account of their unique optical, magnetic,

Received 18 December 2009; in final form 7 March 2010.
Financial support by UGC, India, through project No. F.30-64/2004 (SR) is thankfully acknowledged.
Address correspondence to L. Cindrella, Department of Chemistry, National Institute of Technology, Tiruchirappalli, Tamil Nadu 620015, India. E-mail: cind@nitt.edu

electronic and catalytic properties [1,2]. Pani is a highly promising material for electronic applications due to its combination of electrical conductivity and environmental stability [3–5]. It is expected that the incorporation of inorganic semiconducting nanoparticles in Pani matrices would bring about the synergistic blending of their properties, resulting in materials with attractive electronic properties [6–8]. Metal sulphides with controlled size and shape are gaining immense importance in this context due to their specific and attractive multifunctional properties. Considerable efforts are being devoted to fabricate core-shell colloidal sulphides with custom-specific structural, optical and surface properties [9,10]. Compared to their individual constituents, the core-shell particles exhibit better physical and chemical properties, thereby widening their range of applications [11]. Among the various metal sulphides, nickel sulphide is one of the promising candidates [12–15]. As the size and extent of aggregation of the particles play a significant role in the optical properties, stabilization of the particles in a suitable matrix is essential. The large surface-to-volume ratio in nanocomposites enables an efficient separation of photo-induced charges, which is the important requirement for photovoltaic applications [16,17]. While designing large surface area nanocomposites for highly efficient photoelectrochemical devices, the inclusion of conducting and luminescent boosters in such systems will pave the way for their further enhanced efficiency.

In this article, we report a polymer-controlled in situ growth strategy to prepare the composite films of NiS/MnS core-shell particles embedded in Pani using polyvinyl alcohol (PVA) as the polymer-controller matrix. The progressive improvement in the optical and electronic properties of the composites with each stage of preparation is promising, and the evaluation of the polymer solar cells formed from these materials is reported.

Downloaded At: 15:55 18 January 2011

EXPERIMENTAL

Polyvinyl alcohol (Kemphasol Chemical Ltd.), nickel chloride, cobalt chloride, manganese chloride, aniline hydrochloride and ammonium persulphate (Fischer Ltd.) were used for preparation without any further purification. All chemicals used were of AR grade. Hydrogen sulfide was prepared in the laboratory using Kipp's apparatus. Double-distilled water was used for the preparation of the solutions. The concentration of the solutions was optimized to obtain stable colloidal solutions. The typical preparation is outlined below.

20 ml of 0.1 M of nickel chloride was added to 10% PVA solution followed by the addition of 20 ml of 0.25% cobalt chloride solution, H_2S gas and 20 ml of 2.2% manganese chloride under constant stirring conditions. The colloidal solution obtained was sonicated for 5 min and then added to 25 ml of aniline hydrochloride (0.2 M) solution. 25 ml of ammonium persulphate (0.25 M)

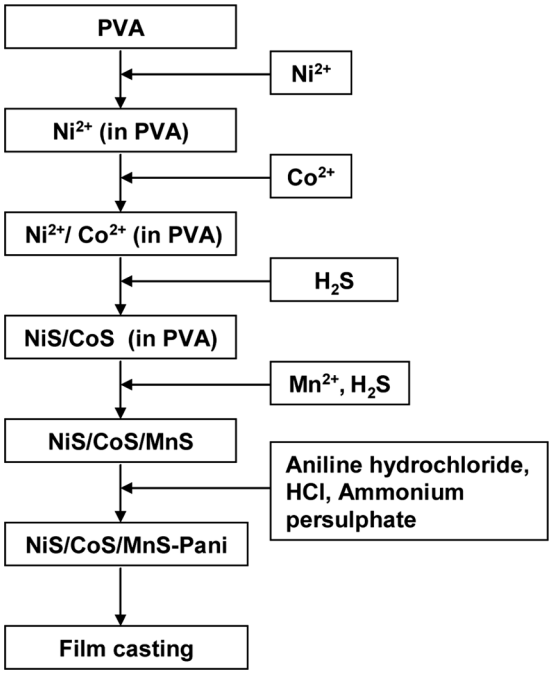

Figure 1: Schematic diagram of the synthesis of NiS:Co/MnS-Pani composite.

Downloaded At: 15:55 18 January 2011

solution was added under constant stirring conditions. The solution was stirred for 30 min to allow the polymerization to complete. From this solution free-standing films of the core-shell composites embedded in Pani were formed by casting. The films were rinsed with dilute hydrochloric acid for the purpose of doping Pani. Pani film was washed with acetone to remove the oligomers. The film was dried at 80°C in an oven and used for further studies. The sequence of steps involved in the synthesis is given in a flow chart (Figure 1).

RESULTS AND DISCUSSION

UV-Visible Spectra

Figure 2 shows the optical absorption spectra of NiS, NiS:Co, NiS:Co/MnS core-shell colloids along with that of Pani and Pani loaded with each stage of colloids. An increase in absorbance is observed for the Co^{2+} doped NiS colloidal particles (Figures 2a, 2b). With the formation of MnS, the absorbance increases further (Figure 2c). For bulk NiS, CoS and MnS, the absorption edges are at 350 nm [18], 400 nm [18] and 310 nm [19], respectively. Blue shift in the absorption edge for NiS (280 nm, Figure 2a) and NiS:Co (255 nm, Figure 2b), from their corresponding bulk values, implies the quantum

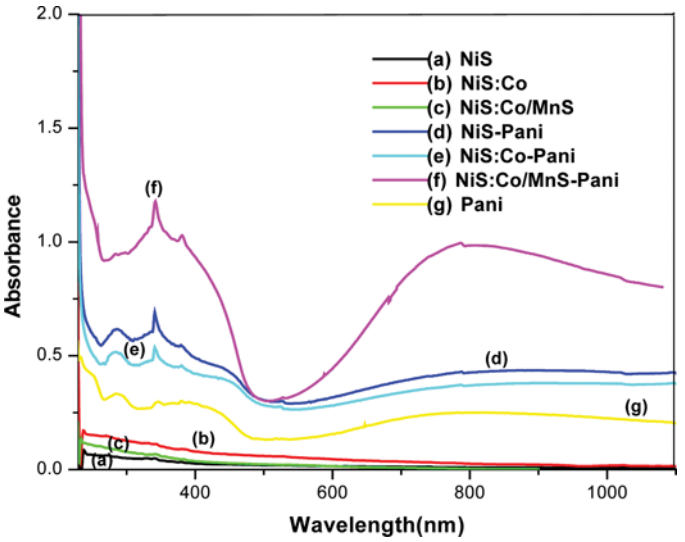

Figure 2: UV-Visible absorption spectra of (a) NiS (b) NiS:Co (c) NiS:Co/MnS (d) NiS-Pani (e) NiS:Co-Pani (f) NiS:Co/MnS-Pani and (g) Pani.

Downloaded At: 15:55 18 January 2011

confinement of the particles [20]. No other exciton peak or another steep edge in the UV region of the optical absorption spectra was observed, indicating the absence of isolated MnS nanoparticles [21]. The absorption spectra of NiS in Pani (Figure 2d), NiS:Co in Pani (Figure 2e) and NiS:Co/MnS in Pani (Figure 2f) are shown in Figure 2. The Pani-colloid composite shows a wide absorption spectrum (Figure 2f) in the UV-visible and near IR regions, much preferred for the photoelectrochemical systems. The absorption spectrum of Pani is also shown for comparison (Figure 2g). The increase in the absorption intensity of Pani with the inclusion of NiS:Co/MnS core-shell is evident from Figure 2. In the absorption spectrum of Pani, the peak at 328 nm is due to the π–π^* transition within the benzenoid segment. The second shoulder-like absorption band at 450 nm is attributed to the doping level of Pani, and the third absorption peak around 800 nm is related to the formation of localized polaron at the backbone of the polymer. The observed three characteristic peaks in the absorption spectra indicate only pure emeraldine salt (ES) formed in the system without the formation of an emeraldine base (EB) or leucoemeraldine base (LB) of Pani. The absorption peaks in the core-shell composite embedded in Pani are due to the synergetic effects of polyaniline and the core-shell materials. The core-shell composite embedded in Pani shows a wide absorption spectrum in the UV-visible and near infrared regions, very favorable for the photoelectrochemical harvesting of solar energy.

Figure 3 shows the Tauc plot for NiS:Co/MnS-Pani. Band gap energy and transition type was derived from mathematical treatment of the data obtained

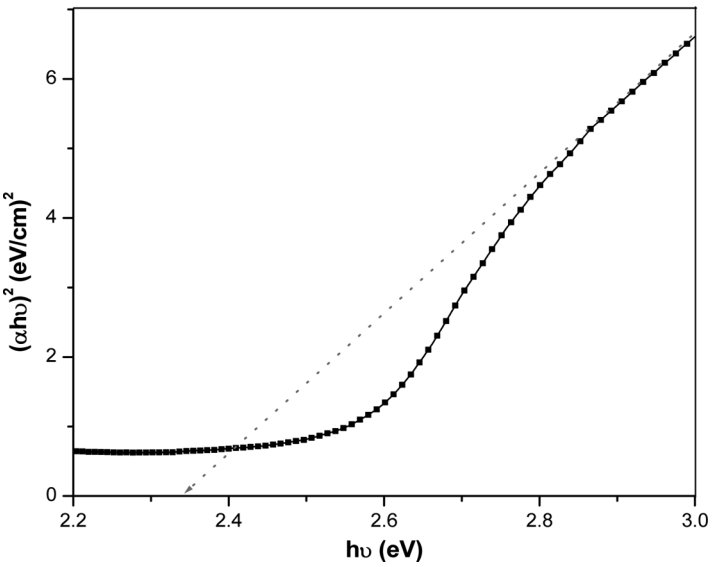

Figure 3: Tauc plot for NiS:Co/MnS-Pani.

Downloaded At: 15:55 18 January 2011

from the optical absorbance vs. wavelength with the following relationship for near-edge absorption:

$$\alpha = \frac{[k(h\nu - E_g)^{n/2}]}{h\nu} \tag{1}$$

where, α is the absorption coefficient (cm^{-1}), h is the Planck's constant; ν is the frequency of radiation (Hz), E_g is the energy band gap (eV) for direct band gap semiconductor, k equals a constant while n carries the value of either 1 or 4. The band gap, E_g, could be obtained from a straight line plot of $(\alpha h\nu)^{2/n}$ as a function of $h\upsilon$. Extrapolation of the line to the base line, where the value of $(\alpha h\nu)^{2/n}$ is zero, will give E_g [22]. If a straight line graph is obtained for $n = 1$, it indicates a direct electron transition between the states of the semiconductor, whereas the transition is indirect if a straight line graph is obtained for $n = 4$. Figure 3 shows the plot of $(\alpha h\nu)^2$ against $h\nu$ for NiS:Co/MnS-Pani. The straight-line behavior testifies a direct transition of the band structure. Extrapolation of the straight portion of the graph to $\alpha = 0$ gives a band gap energy of 2.34 eV for NiS:Co/MnS-Pani.

Photoluminescence

The PL spectra for NiS, CoS, MnS, NiS:Co, NiS:Co/MnS, and NiS:Co/MnS-Pani core-shell particles are shown in Figure 4 at an excitation wavelength of 300 nm. The PL spectrum of NiS (Figure 4a) shows the blue band at 431 nm (2.87 eV) due to the band-edge emission, with about 1.07 eV blue shift

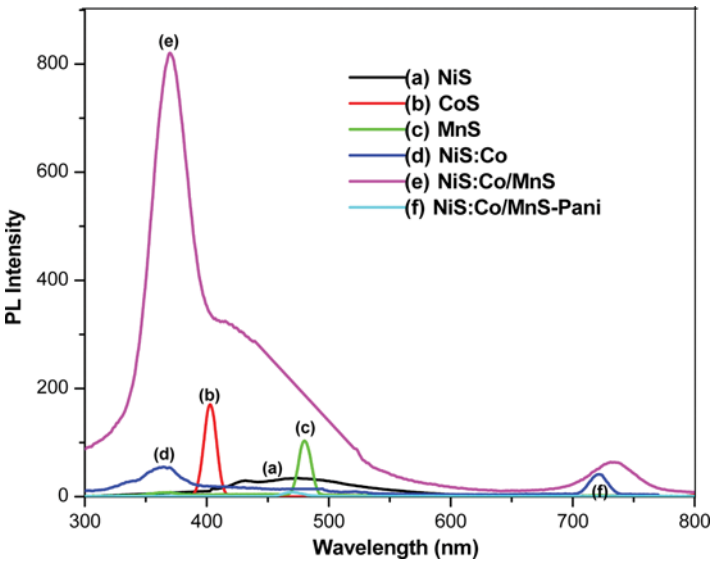

Figure 4: Photoluminescence emission spectra of (a) NiS (b) CoS (c) MnS (d) NiS:Co (e) NiS:Co/MnS and (f) NiS:Co/MnS-Pani.

compared to the bulk crystal (1.8 eV) [23] due to the quantum size effect. The PL spectrum for CoS (Figure 4b) shows the near band edge intense emission at 400 nm and a weak emission at 810 nm (not shown). The PL spectrum for MnS (Figure 4c) shows the near band edge intense emission at 480 nm and a weak emission at 364 nm. while NiS:Co (Figure 4d) exhibits a blue shifted emission peak at 370 nm. The photoluminescence of NiS:Co/MnS (Figure 4e) exhibits a strong and broad peak centered at about 368 nm with increased photoluminescence emission. The increase in PL intensity with the inclusion of MnS provides evidence for the formation of core-shell nanoparticles rather than a mixture of NiS and MnS nanoparticles. For the physically mixed system of NiS and MnS, the PL intensity would register a decrease at their characteristic emission peaks, whereas for the core/shell formation the PL intensity increases [24]. While the doping of NiS with Co has blue shifted the PL peak, shell formation with MnS has enormously increased the emission intensity over the visible range and hence acts as the booster for the incident visible light very useful for the photoelectrochemical systems. The addition of Pani suppresses the photoluminescence (Figure 4f). The low values of PL intensity at all wavelengths in core-shell-Pani are due to the fact that Pani is nonfluorescent and it disallows the recombination of photogenerated charges.

XRD Studies

X-ray powder diffraction (XRD) analysis was carried out to investigate the phase of the NiS:Mn/CdS-Pani composite. A typical XRD pattern of the film is

Downloaded At: 15:55 18 January 2011

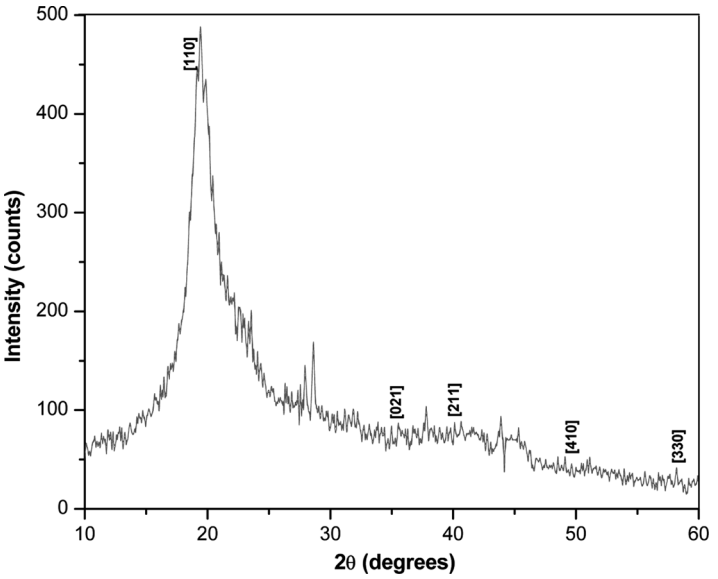

Figure 5: XRD pattern of NiS:Mn/CdS core-shell embedded Pani film.

Downloaded At: 15:55 18 January 2011

shown in Figure 5. Particle size of about 96 nm was evaluated by Scherrer equation. Peaks have been indexed and suggest that the core material formed is NiS with rhombohedral crystal structure with cell parameters, $a = 9.620$ Å and $c = 3.149$ Å, which are close to the data in JCPDS card no. 12-0041 and also reported by Qingtao Pan et al. [23]. Separate peaks characteristic of MnS or CdS are not observed. The presence of a small foreign ion inclusion [25] or a shell layer over the core does not affect the XRD peaks of the core particles [26,27].

SEM Analysis

Figure 6 shows the scanning electron micrograph of NiS:Co/MnS-Pani film at three different magnifications. The particles are circular to oval in shape with the size ranging from well under 200 nm. Larger particles revealed dull interiors and bright peripherals highlighting the containment of luminescence to each of the particles. As attempts to obtain higher resolution SEM damaged the polymer matrices, we could not take HRSEM. The uniform distribution of the core/shell particles is evident. SEM provides evidence for the stabilization of the core/shell particles-Pani composite by its periodic arrangement. Nanoscale aggregation of the particles is also observed from SEM images. The periodic arrangement of the semiconductor particles in a conducting matrix facilitates its photoelectrochemical activity.

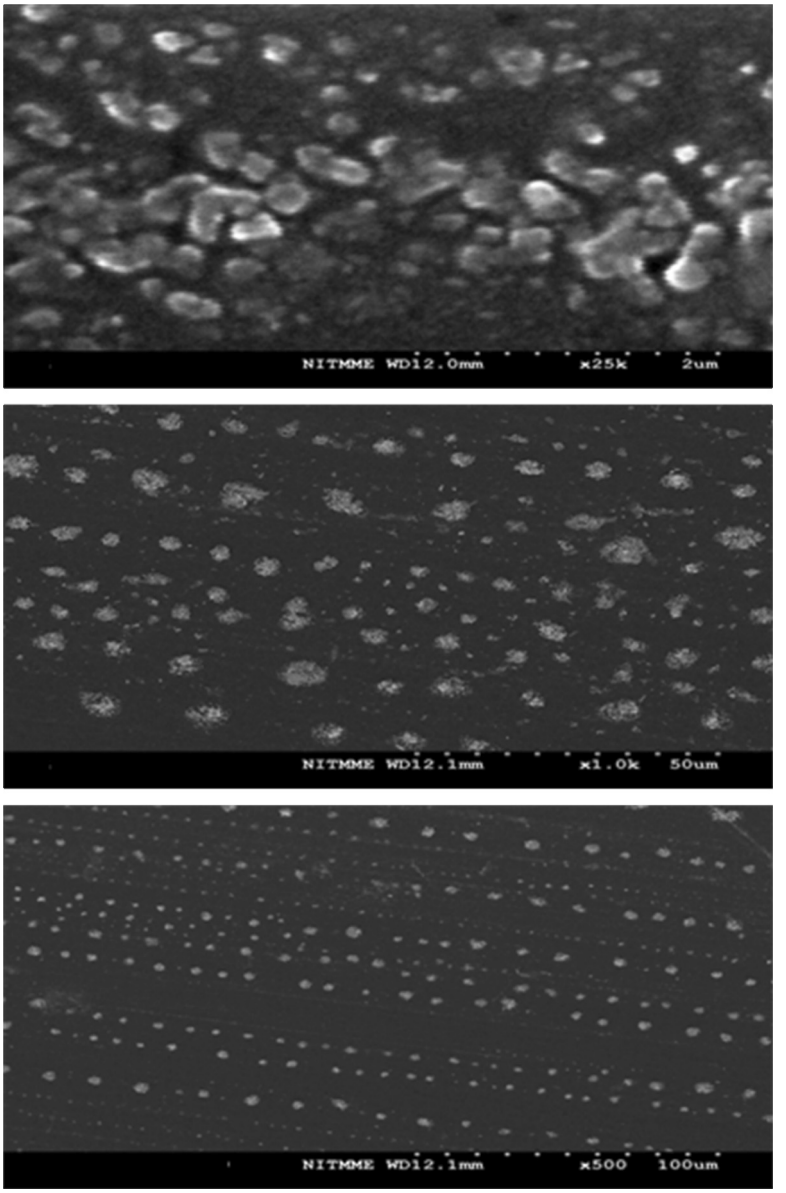

Figure 6: Scanning electron micrograph of NiS:Co/MnS core-shell particles embedded Pani film at three different magnifications.

Mott-Schottky Plot

The Mott-Schottky plot is constructed of the inverse square of space charge layer capacitance measured at a fixed frequency of 10000 Hz as a function of potential [28,29]. The Mott-Schottky plot (Figure 7) shows a positive

Downloaded At: 15:55 18 January 2011

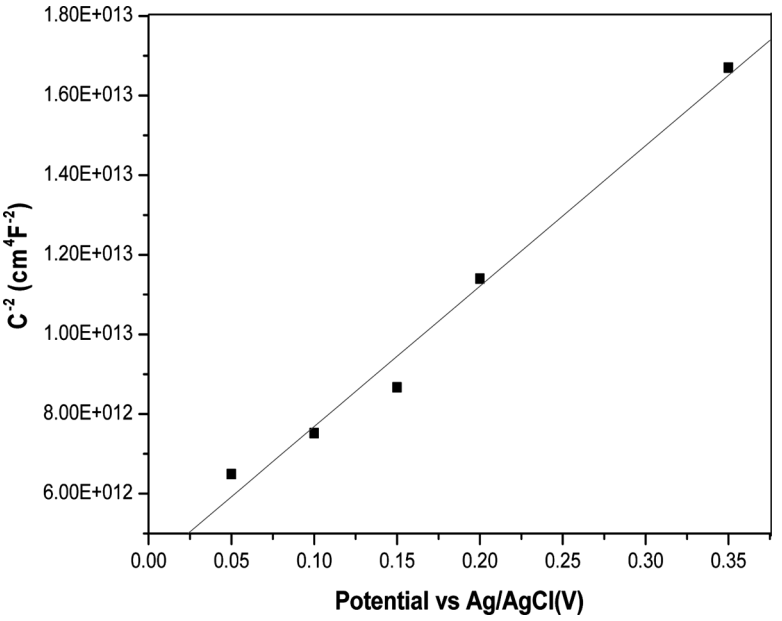

Figure 7: Mott Schottky plot of NiS:Co/MnS core-shell particles embedded Pani film.

Downloaded At: 15:55 18 January 2011

slope for the NiS:Co/MnS core-shell particle embedded Pani film indicating a typical n-type characteristic of the film. The paramagnetic characteristic of this composite material was also confirmed by the magnetic susceptibility measurement using a Sherwood Auto MSB meter. The Mott-Schottky plot shows a positive slope for the NiS:Co/MnS core-shell particle embedded Pani film, indicating a typical n-type of the semiconductor. The flat-band potential (E_{fb}) is inferred from the intersection of the plot with the x-axis as 0.025 V. The carrier density of the core-shell-Pani composite is evaluated from the plot as 3.99×10^{16}.

AC Impedance

Features in the impedance spectrum of electrochemical systems are related to physicochemical processes, occurring in the system when an electric current passes through it [30,31]. Charge transfer resistance (R_{ct}) is a characteristic quantity for an electrode reaction indicative of electron transfer kinetics. Thus a large charge-transfer resistance indicates a slow reaction. The curvature of the Nyquist plot in Figure 8 at high frequencies represents the double-layer capacitance in parallel with the charge transfer resistance. From the AC impedance spectrum, the charge transfer resistance of the film was found to be 1644 Ω. The equivalent circuit for NiS:Co/MnS-Pani electrode is shown as inset.

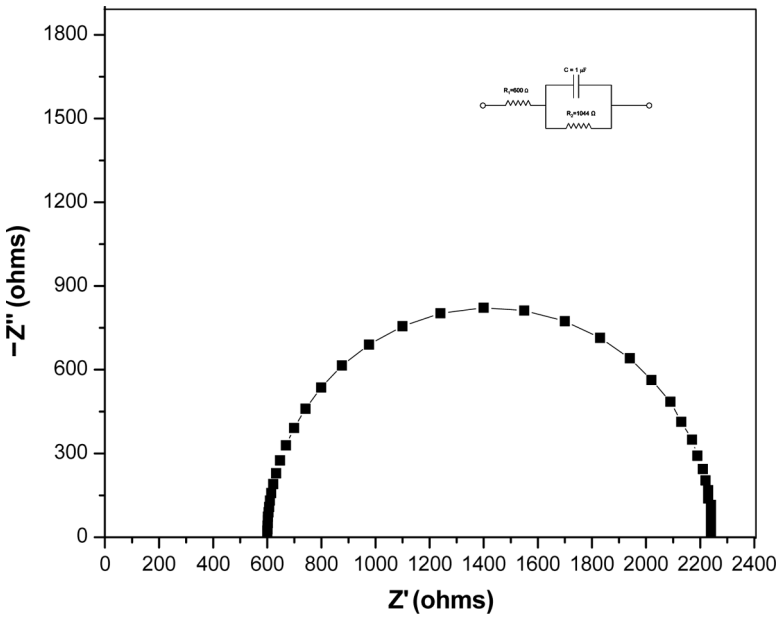

Figure 8: AC Impedance spectrum of NiS:Co/MnS core-shell particles embedded Pani film (Inset: equivalent circuit).

Conductivity Measurement

Figure 9 shows the films of NiS:Co/MnS (a) and NiS:Co/MnS-Pani (b) the conductivity of the core-shell particles embedded Pani film was 0.03 S/cm as evaluated by the four probe method.

I-V Characteristics

A photoelectrochemical cell with an active area of 2 cm^2 was fabricated with NiS:Co/MnS-Pani film (n-type) as the anode and pristine Pani film

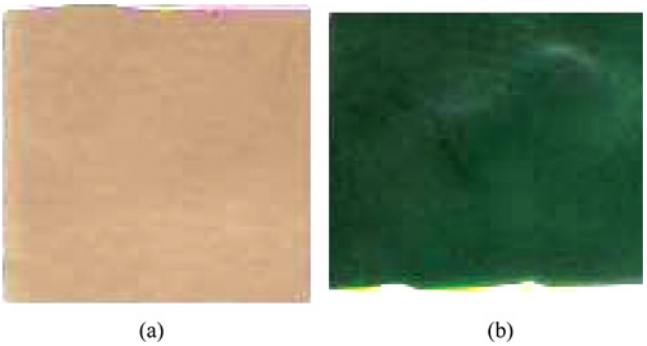

Figure 9: Photographs of (a) NiS:Co/MnS core-shell composite film and (b) NiS:Co/MnS core-shell embedded Pani film.

Downloaded At: 15:55 18 January 2011

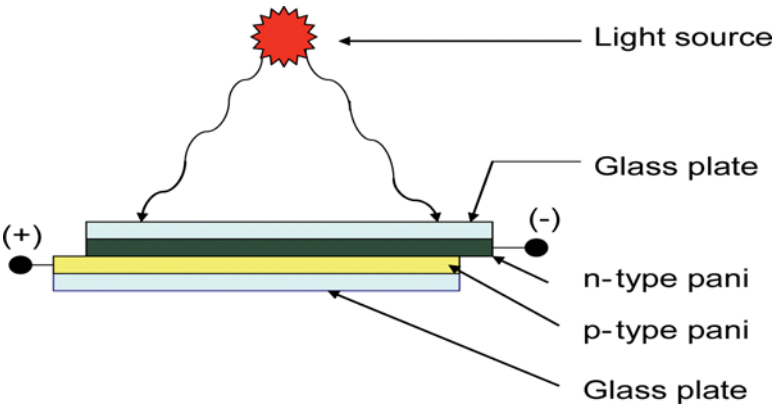

Figure 10: Schematic diagram of solid state solar cell assembled.

Downloaded At: 15:55 18 January 2011

(p-type) as the cathode. Pani has been successfully used as a hole conductor material to fabricate the solid-state dye-sensitized TiO_2 solar cells [32–37]. Figure 10 shows the schematic diagram of solid-state solar cell assembled. The current voltage characteristics of the cell was evaluated (Figure 11) with a white light source of intensity 15 mW/cm^2. P_{max} was found to be 0.188 mW/cm^2 while the open circuit voltage (V_{oc}) and short circuit current (I_{sc}) are 382 mV and 0.14 mA/cm^2, respectively. The calculated cell efficiency and fill factor are 1.25% and 0.36, respectively.

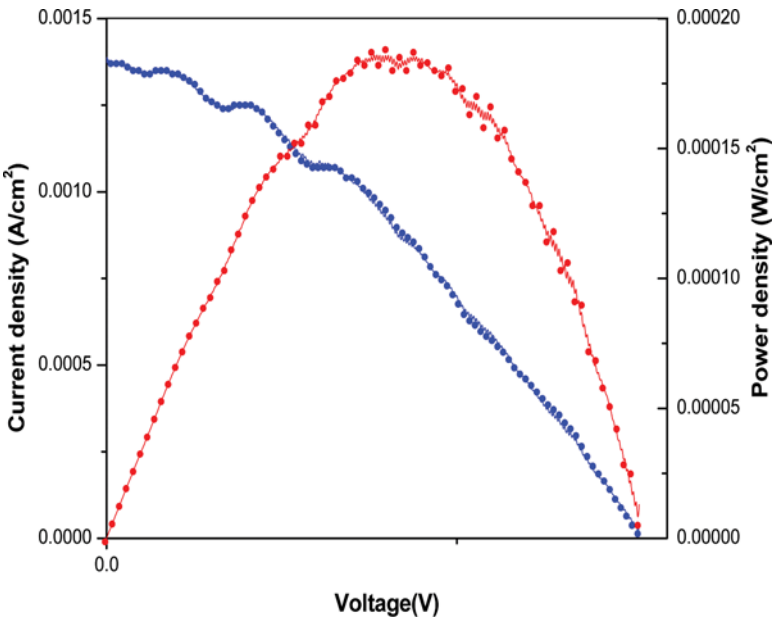

Figure 11: Solar cell performance of solid state solar cell assembled with NiS:Co/MnS-Pani (n-type) and pristine Pani (p-type).

Energy Diagram and Mechanism

Figure 12 shows the energy level diagram for photoinduced electron transfer between NiS:Co/MnS-Pani (n-type) and pristine Pani (p-type). The energy gap of NiS:Co/MnS-Pani and Pani may be estimated from their absorption edges (Figure 2). The band energy diagram has been developed by converting the energy levels of the semiconductors referring to an energy scale using the equation, $E(eV) = -4.5 - E(V)$, where the electrochemical potential is related to the standard hydrogen electrode (NHE) [38, 39]. The band gaps and the energy of the electronic levels of core-shell composite and Pani allow charge separation across the conducting polymer|nanoparticle interface. Upon photoexitation, the excited electron will be transferred from the conducting polymer to the nanoparticle. The mechanism of the photo excitation process leading to the photoinduced charge separation [40] between the donor (D) and acceptor (A) could be summarized as below.

$$D + A \rightarrow D^* + A \text{ (excitation of the donor)}$$
$$D^* + A \rightarrow (D\text{---}A)^* \text{ (excitation delocalized on the donor-acceptor system)}$$
$$(D\text{----}A)^* \rightarrow (D^{\delta+}\text{----}A^{\delta-})^* \text{ (partial charge transfer)}$$

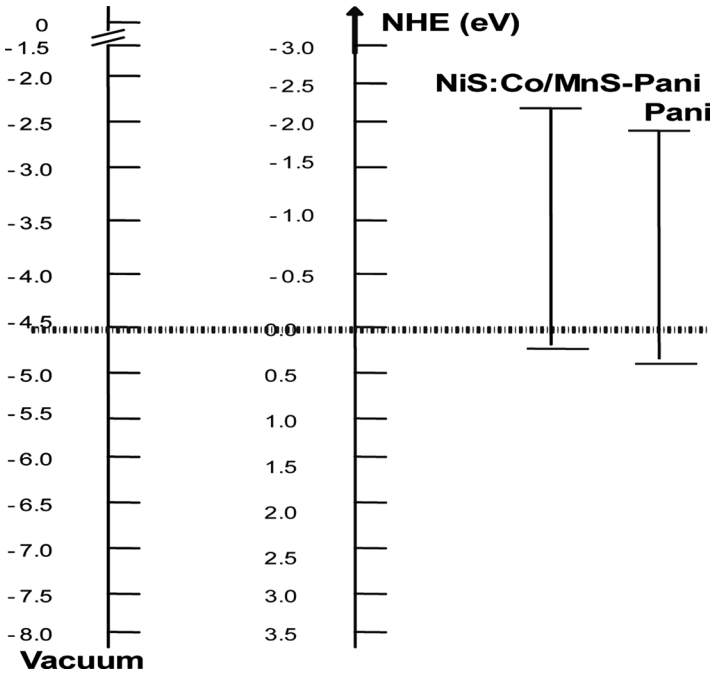

Figure 12: Schematic energy diagram for photoinduced electron transfer between NiS:Co/MnS-Pani (n-type) and pristine Pani (p-type).

Downloaded At: 15:55 18 January 2011

$$(D^{\delta+}\text{---}A^{\delta-})^* \rightarrow (D^{+\cdot}\text{---}A^{-\cdot})^* \text{ (ion-radical pair formed)}$$
$$(D^{+\cdot}\text{----}A^{-\cdot})^* \rightarrow D^{+\cdot}\text{----}A^{-\cdot} \text{(charge separation)}$$

In a hybrid film of conducting polymer and high electron affinity-nanoparticles, the nanoscale confined semiconductor particles favor the delocalization of the excitation on Pani. The embedded core shells form the acceptor system, Pani matrix forms the donor part of the exciton. The periodically embedded nanoparticles with the electrons and the continuous conductive matrix of Pani with the holes provide the effective charge separation to be tapped through the external circuit.

CONCLUSION

A novel photoactive composite film of conducting polyaniline with fluorescent boosters is prepared. Room-temperature synthesis of a photoactive n-type semiconductor material based on core-shell structures in a Pani matrix has been optimized and reported. The UV-visible absorption and emission spectra revealed the step-wise spectral modifications effected by the preparation method. The scanning electron micrographs revealed core-shell structure and their periodic arrangement in the polymer matrix. The conductivity and carrier density of this material is promising for photoelectrochemical applications. A solid-state solar cell has been fabricated and evaluated. This configuration, with no liquid electrolyte, is easy for scale-up and effective for installation at any angle to harness maximum solar radiation.

Downloaded At: 15:55 18 January 2011

REFERENCES

[1] Mayer, A. B. R. *Mater. Sci. Eng.* **C6**, 155 (1998).

[2] Caseri, W. *Macromol. Rapid Commun.* **21**, 705 (2000).

[3] Syed, A. A., and Denesan, M. K. *Talanta.* **38**, 815 (1991).

[4] Kang, E. T., Neoh, K. G., and Tan, K. L. *Prog. Polymer. Sci.* **23**, 277 (1998).

[5] Hutten, P. F., and Hadziioannou, G. (1997) *Handbook of Organic Conductive Molecules and Polymers*, *3*, John Wiley & Sons, New York, p. 2.

[6] O'Regan, B., and Grätzel, M. *Nature* **353**, 737 (1991).

[7] Wang, Y., and Herron, N. *Chem. Phys. Lett.* **200**, 71 (1992).

[8] Dabbousi, B. O., Bawendi, M. G., Onitsuka, O., and Rubner, M. F. *Appl. Phys. Lett.* **66**, 1316 (1995).

[9] Loukanov, A. R., Dushkin, C. D., Papazova, K. I., Kirov, A. V., Abrashev, M. V., and Adachi, E. *Colloid Surf. A: Physicochem. Eng. Aspects.* **245**, 9 (2004).

[10] Hota, G., Jain Shikha, J., and Khilar, K. C. *Physicochem Eng Aspect.* **232**, 119 (2004).

[11] Viswanadh, B., Tikku, S., and Khilar, K. C. *Colloid Surf. A: Physicochem. Eng. Aspects* **298**, 149 (2007).

[12] Han, S. C., Kim, K. W., Ahn, H. J., Ahn, J. H., and Lee, J. Y. *J. Alloy Comp.* **361**, 247 (2003).

[13] Yermakov, Y. I., Startsev, A. N., and Burmistrov, V. A. *Applied Catalysis* **11**, 1 (1984).

[14] Tanaka, K. I., and Okuhara, T. *Catal. Rev. Sci. Eng.* **15**, 249 (1977).

[15] Jasinski, R., and Burrows, B. J. *Electrochem. Soc.* **116**, 422 (1969).

[16] Wang, Y., and Herron, N. *J. Luminesc.* **70**, 48 (1996).

[17] Wang, Y. *Studies Surf. Sci. Catal.* **103**, 277 (1996).

[18] Sohrabnezhad, Sh., Pourahmad, A., Sadjadi, M. S., and Sadeghi, B. *Physica E.* **40**, 84 (2008).

[19] Nosipho, M., Coville, N. J., Ray, S. S., and Molot, M. J. *Physica B: Condensed Matter.* (Article in Press). (2009).

[20] Malik, A. Z., Brien, P. O., and Revaprasadu, N. *J. Mater. Chem.* **11**, 2382 (2001).

[21] Saraswathi Ammaa, B., Manzoorb, K., Ramakrishnaa, K., and Pattabi, M. *Mater Chem. Phys.* **112**, 789 (2008).

[22] Kassim, A., Tee, T. W., Sharif, A. M., Abdullah, D. Y., Haron, M. J., Min, H. S., and Saravanan, N. *J. Chil. Chem. Soc.* **54**, 256 (2009).

[23] Pan, Q., Huang, K., Ni, S., Yang, F., and He, D. *Mater Res Bull.* **43**, 1440 (2008).

[24] Lu, S. Y., Wu, M. L., and Chen, H. L. *J. Appl. Phys.* **93**, 5789 (2003).

[25] Kortan, A. R., Hull, R., Opila, R. L. M. G., Bawendi, M. G., Steigerwald, M. L., Carroll, P. J., and Brus, L. E. *J. Am. Chem. Soc.* **112**, 1327 (1990).

[26] Yang, H., Holloway, P. H., Cunnigham, G., and Schanze, K. S. *J. Chem. Phys.* **121**, 10233 (2004).

[27] Peng, X., Schlamp, M. C., Kadavanich, A. V., and Alivisatos, A. *J. Am. Chem. Soc.* **119**, 7019 (1997).

[28] Cordon, F., and Gomes, W. P. *J. Phys. D: Appl. Phys.* **11**, 63 (1978).

[29] Geldermann, K., Lee, L., and Donne, S. W. *J. Chem. Educ.* **84**, 685 (2007).

[30] Bard, A. J., and Faulkner, L. R. (1980). *Electrochemical Methods: Fundamentals and Applications*, Wiley, New York.

[31] Macdonald, J. R. (2000). *Impedance Spectroscopy: Emphasizing Solid Materials and Systems*, Wiley, New York.

[32] Liu, Z., Zhou, J., Xue, H., Shen, L., Zang, H., and Chen, W. *Synthetic Metals* **156**, 721 (2006).

[33] Tan, S. X. J., Zhai, J., Wan, M. X., Jiang, L., and Zhu, D. B. *Synthetic Metals* **137**, 757 (2003).

[34] Wu, W. J., Zhan, W. H., Hua, J. L., and Tian, H. *Research on Chemical Intermediates* **34**, 241–248 (2008).

[35] Tan, S., Zhai, J., Xue, B., Wan, M., Meng, Q., Li, Y., Jiang, L., and Zhu, D. *Langmuir* **20**, 2934 (2004).

Downloaded At: 15:55 18 January 2011

[36] Paul, G., Bhaumik, K. A., Patra, A. S., and Bera, S. K. *Mat. Chem. Phys.* **106**, 360 (2007).

[37] Sapurina, I. Y., Gribanov, A. V., Mokeev, M. V., Zgonnik, V. N., Trchova, M., and Stejskal, J. *J. Phy. Solid State* **44**, 574 (2006).

[38] Greenham, N. C., Peng, X., and Alivisatos, A. P. *Phys. Rev. B.* **54**, 17628 (1996).

[39] Santos, M. J. L., Ferreira, J., Radovanovic, E., Romano, R., Alves, O. L., and Girotto, E. M. *Thin Solid Films*, **517**, 5523 (2009).

[40] Sariciftci, N. S., and Heeger, A. J. (1997) *Handbook of Conductive Molecules and Polymers*, John Wiley and Sons, New York.

Downloaded At: 15:55 18 January 2011